Supplementary Data

Spatio-temporal proteomic profiling of SARS-CoV-2 replication organelles

Doil Yoon1,2,4, Sunghan Lee1,2,4, Yun-Bin Lee3, Jeesoo Kim1,2, Jong-Seo Kim1,2, Hyun-Woo Rhee*2,3, V. Narry Kim*1,2

1 Center for RNA Research, Institute for Basic Science, Seoul 08826, Korea
2 School of Biological Sciences, Seoul National University, Seoul 08826, Korea
3 Department of Chemistry, Seoul National University, Seoul 08826, Korea
4 These authors contributed equally
* Correspondence and lead contact: narrykim@snu.ac.kr, rheehw@snu.ac.kr

Tables

Supplementary Table 1

Supplementary table listing oligonucleotides, siRNAs, and sgRNA sequences and antibodies used in this study.

Supplementary Table 2

Supplementary table of mass shift of peptides detected in SARS-CoV-2 RO proximity profiling.

Supplementary Table 3

Supplementary table of mass shift of peptides detected in HCoV-OC43 RO proximity profiling.

Supplementary Table 4

Supplementary table of proteins detected in SARS-CoV-2 and HCoV-OC43 RO proximity profiling.

Supplementary Figure 1-5.

Supplementary Table 1. Supplementary table listing oligonucleotides, siRNAs, and sgRNA sequences and antibodies used in this study.

1. Oligonucleotides

Name	Sequence
SARS2 gRNA qPCR_F	CAGAGAGCTAGGTGTTGTAC
SARS2 gRNA qPCR_R	AAGCACGTAGTGCGTTTATC
SARS2 sgRNA (N) qPCR_F	CAGCGTTCTTCGGAATGTCG
SARS2 sgRNA (N) qPCR_R	AGGCTTGAGTTTCATCAGCC
OC43 gRNA qPCR_F	CACTGTTGCTGGTGTTTCCA
OC43 gRNA qPCR_R	GCGGCGTAACATATCATCCC
STAU1_qPCR_F	GAGTACACGCTCCTCACAGA
STAU1_qPCR_R	CCTTCTGCAGTGTGGTTTCC
GAPDH_F	CAAGAAGGTGGTGAAGCAGGC
GAPDH_R	CATACCAGGAAATGAGCTTGAC

2. siRNAs

siRNA screening (ON-TARGETplus SMARTpool siRNAs, Horizon Discovery)

Name	Cat. no
Non-targeting control	D-001810
siEIF5A	L-015739
siFAM120A	L-014186
siPEBP1	L-019679
siSND1	L-010657
siSTAU1	L-011894
siEIF4H	L-013054
siHSPA5	L-008198
siPTCD3	L-016957
siCKAP4	L-012755
siIGF2BP1	L-003977
siPPIA	L-004979

Individual siRNA (Bioneer)

Name	Sequence (or Cat no.)
Non-targeting control	D-001810
siSTAU1_1	CUGUGUUGCUUUUGAUGUU=tt
	AACAUCAAAAGCAACACAG=tt

siSTAU1_2	UGAACGAGUAAAGCCUAGA=tt
	UCUAGGCUUUACUCGUUCA=tt

3. sgRNAs

Name	Sequence
sgNC	GCACTACCAGAGCTAACTCA
	TGAGTTAGCTCTGGTAGTGC
sgSTAU1_#1	TTTGTGACCAAGGTTTCGGT
	ACCGAAACCTTGGTCACAAA
sgSTAU1_#2	GATCAATCCGATTAGCCGAC
	GTCGGCTAATCGGATTGATC
sgG3BP1	TGTCCGTAGACTGCATCTGC
	GCAGATGCAGTCTACGGACA
sgG3BP2	TCTGGTTTAGCTTCGACTCT
	AGAGTCGAAGCTAAACCAGA

4. Antibodies

Name	Cat no.	Company
K1 monoclonal antibody	10020500	English and Scientific Consulting Kft
Normal mouse IgG	sc-2025	Santa Cruz biotechnology
Goat Anti-Mouse IgG (H+L)	115-035-146	Jackson ImmunoResearch
Alexa Fluor 594 goat anti-mouse IgG(H+L)	A-11032	Invitrogen
Alexa 594 Donkey anti-rabbit IgG (H+L)	A-21207	Invitrogen
Alexa Fluor 488 goat anti-rabbit IgG(H+L)	A-11034	Invitrogen
Alexa Fluor 488 donkey anti-Mouse IgG (H+L)	A-21202	Invitrogen
Anti-SND1	Ab65078	Abcam
Anti-STAU1	14225-1-AP	ProteinTech
Anti-G3BP1 (IF, Rb)	61559	Cell Signaling technology
Anti-G3BP (IF, Ms)	611126	BD Bioscience
Anti-G3BP1 (WB)	sc-365338	Santa Cruz
Anti-G3BP2	ab86135	Abcam
Anti-SARS-CoV-2 nsp3 Antibody	NBP3-07966	Novus Biologicals
GAPDH	sc-32233	Santa Cruz biotechnology

Supplementary Figures

Supplementary Figure 1. Quality control and validation of the RO proximity profiling

a-b, Western blot analysis using streptavidin-HRP (a) and Coomassie staining (b) of protein lysates after proximity labeling in SARS-CoV-2-infected A549-ACE2 cells. Samples were collected at 0 and 24 hpi and labeled using either the dsRNA-specific K1 antibody or a mouse IgG control.
c, Scatter plots showing the correlation of protein intensities between three biological replicates of SARS-CoV-2-infected samples for each experimental condition.
d-e, Western blot analysis using streptavidin-HRP (d) and Coomassie staining (e) of protein lysates after proximity labeling in HCoV-OC43-infected HCT-8 cells.
f, Scatter plots showing the correlation of protein intensities between three biological replicates of HCoV-OC43-infected samples for each experimental condition.
g-h, Mass shift analysis of peptides identified in SARS-CoV-2-infected samples (g) and HCoV-OC43-infected samples (h) using an open search. A distinct peak at +331 Da, corresponding to the mass of DBP, confirms successful labeling.

Supplementary Figure 2. Functional characterization of the SARS-CoV-2 RO proteome

a, GO enrichment analysis of the SARS-CoV-2 RO proximity proteome. The circle size represents the degree of enrichment, and the x-axis indicates the $-\log_{10}$(adjusted p-value). P-values were calculated by Fisher's exact test with multiple testing adjustments.
b-f, GO enrichment analysis for five major functional clusters from the RO proximity proteome depicted in Fig. 2a.
g, An enrichment heatmap showing the major Gene Ontology (GO) terms identified in each cluster of the SARS-CoV-2 24 hpi RO proximity proteome. Each GO term was evaluated for enrichment across groups using a hypergeometric test, and the resulting p-values were corrected for multiple comparisons using FDR adjustment.

Supplementary Figure 3. Systematic profiling of the HCoV-OC43 RO proximity proteome

a, Distribution of peptide modification across samples, showing the proportion of peptides with endogenous biotin (green) or DBP (blue) modifications identified by open search.

b, Subcellular localization profile of the HCoV-OC43 RO proximity proteome.
c, GO enrichment analysis of the HCoV-OC43 RO proximity proteome. The circle size represents the degree of enrichment, and the x-axis indicates the $-\log_{10}$(adjusted p-value).
d, Functional interaction network of the SARS-CoV-2 RO proximity proteome, visualized using STRING interaction scores. Node size is proportional to the number of interacting partners and edge thickness corresponds to the confidence score of the interaction.
e, Heatmap quantifying the protein overlap between the functional clusters of the SARS-CoV-2 and HCoV-OC43 RO proximity proteomes. The number of overlapping proteins were divided by the total number of proteins in each cluster of SARS-CoV-2 and HCoV-OC43 and multiplied by 100.
f-g, Volcano (f) and violin plots (g) illustrating the enrichment of a list of antiviral proteins (highlighted in red) in the HCoV-OC43 K1 samples compared to IgG samples. Statistical significance was determined using a one-sided Mann–Whitney U test (**$p < 0.01$).
h-i, GO enrichment analysis of the SARS2-enriched and OC43-enriched proteins. The circle size represents the degree of enrichment, and the x-axis indicates the $-\log_{10}$(adjusted p-value).

Supplementary Figure 4. Stress granule protein dynamics at the SARS-CoV-2 RO

a, Composition of protein groups within major GO terms identified from the SARS-CoV-2 RO proximity proteome clusters shown in Fig. 2a.
b, Bar chart illustrating the $\log_2$ fold-change of stress granule proteins at the RO between 24 hpi and 5 hpi. Negative values indicate depletion from the RO as the infection progresses.
c-d, Representative immunofluorescence images of SARS-CoV-2-infected 293T-ACE2 (c) and HCoV-OC43-infected HCT-8 (d) at 5 hpi, showing localization of G3BP1 and dsRNA.

Supplementary Figure 5. Functional analysis of the viral RNA-interacting RO proteome of SARS-CoV-2

a, RBP2GO score of the viral RNA-interacting RO proximity proteome of SARS-CoV-2.
b, Effect of viral RNA-interacting RO-proximal protein depletion on N subgenomic RNA in SARS-CoV-2-infected cells (48 hpi, MOI = 0.1). Statistical significance was determined using a two-sided t-test with multiple testing adjustments, with *$p < 0.05$, **$p < 0.01$, and ***$p < 0.001$.

Supplementary Figure 1

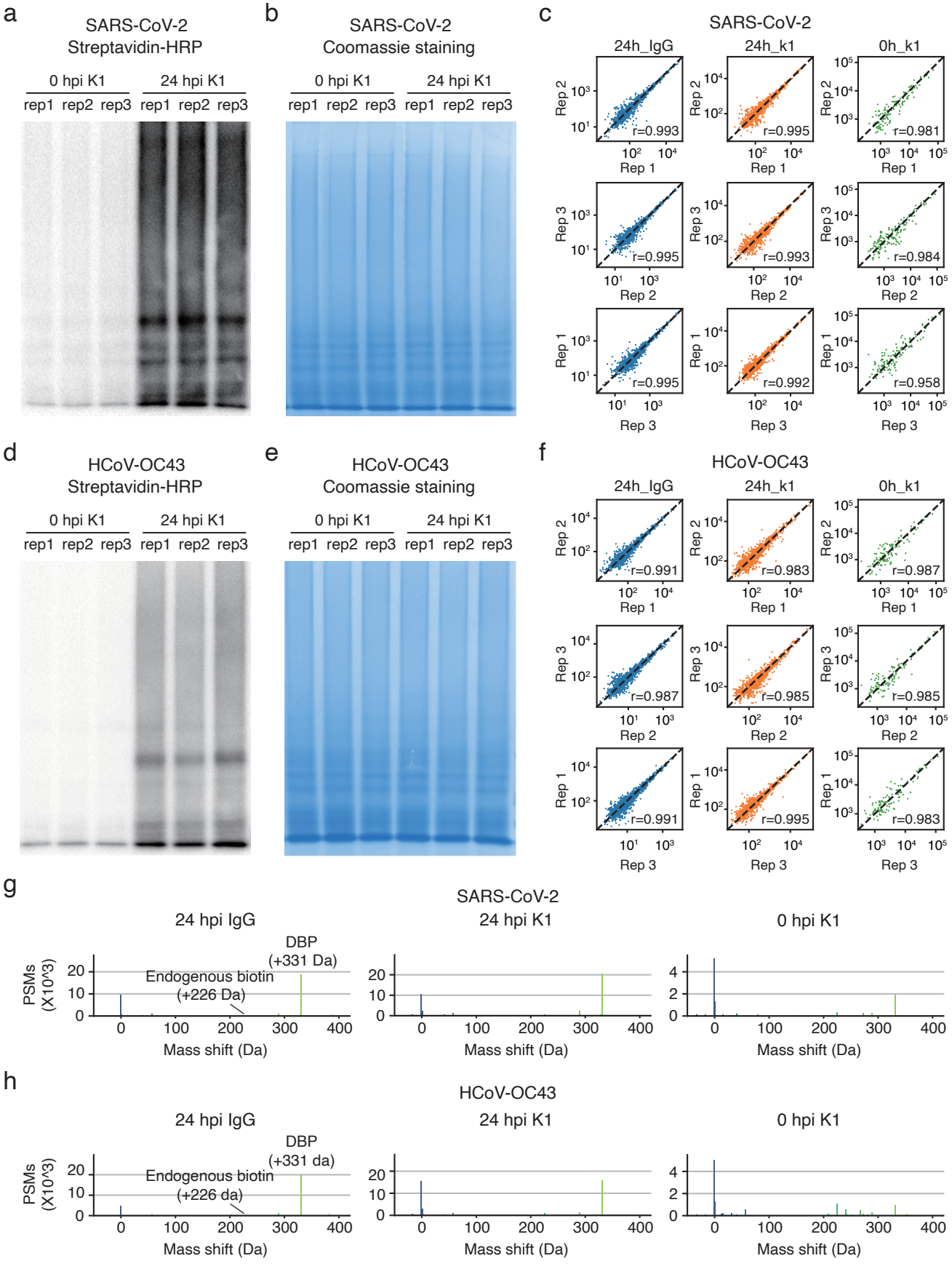

Supplementary Figure 2

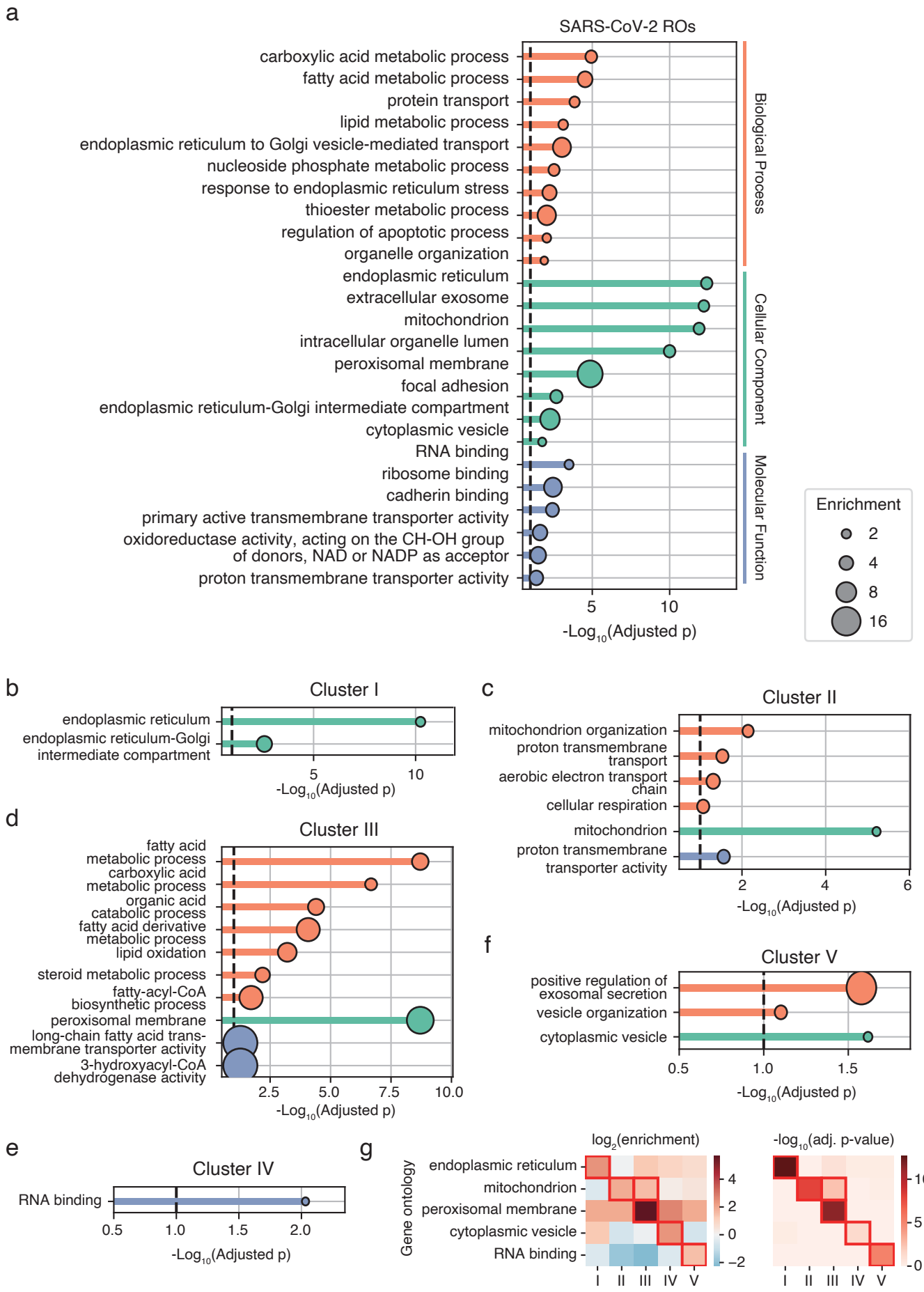

Supplementary Figure 3

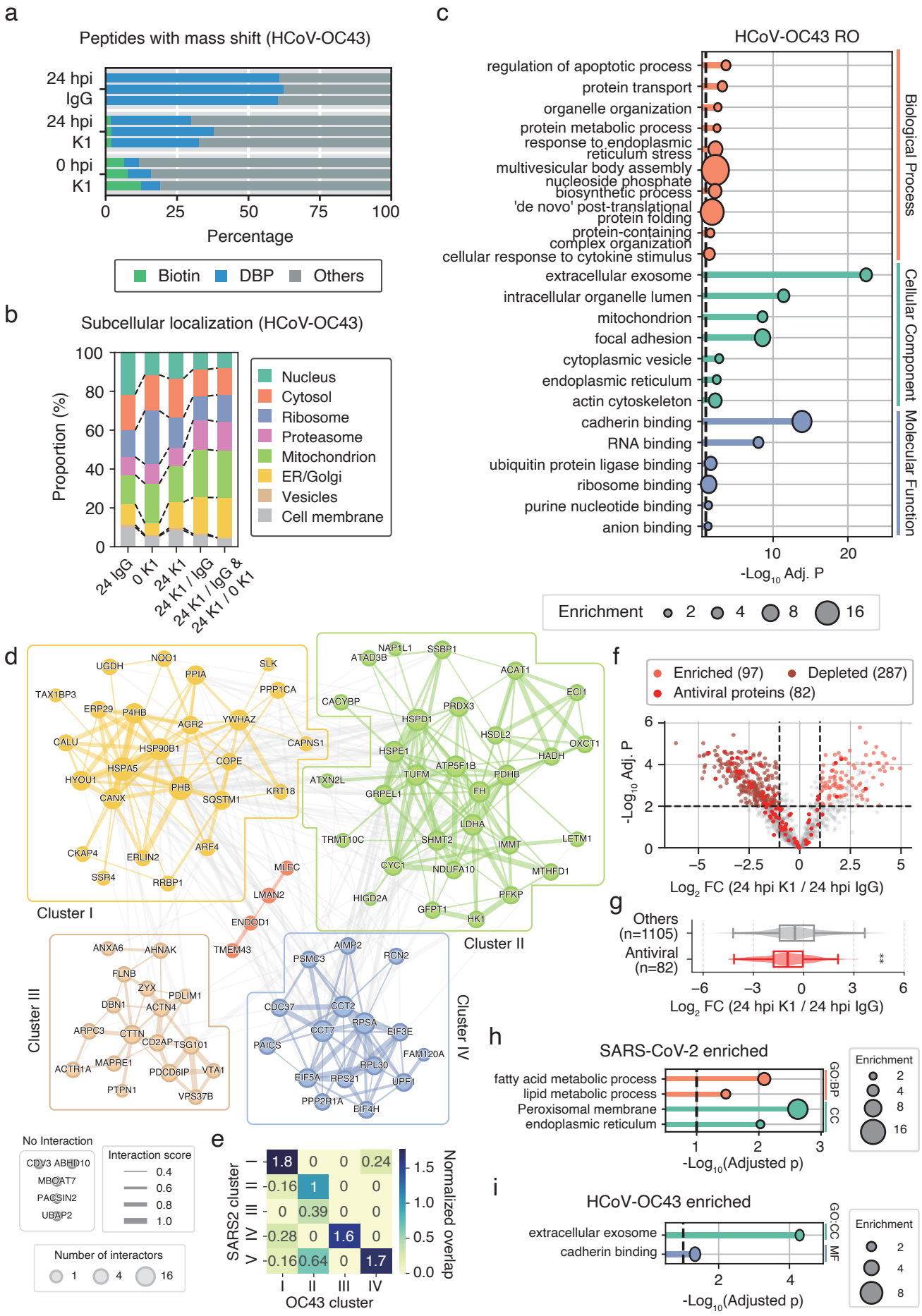

Supplementary Figure 4

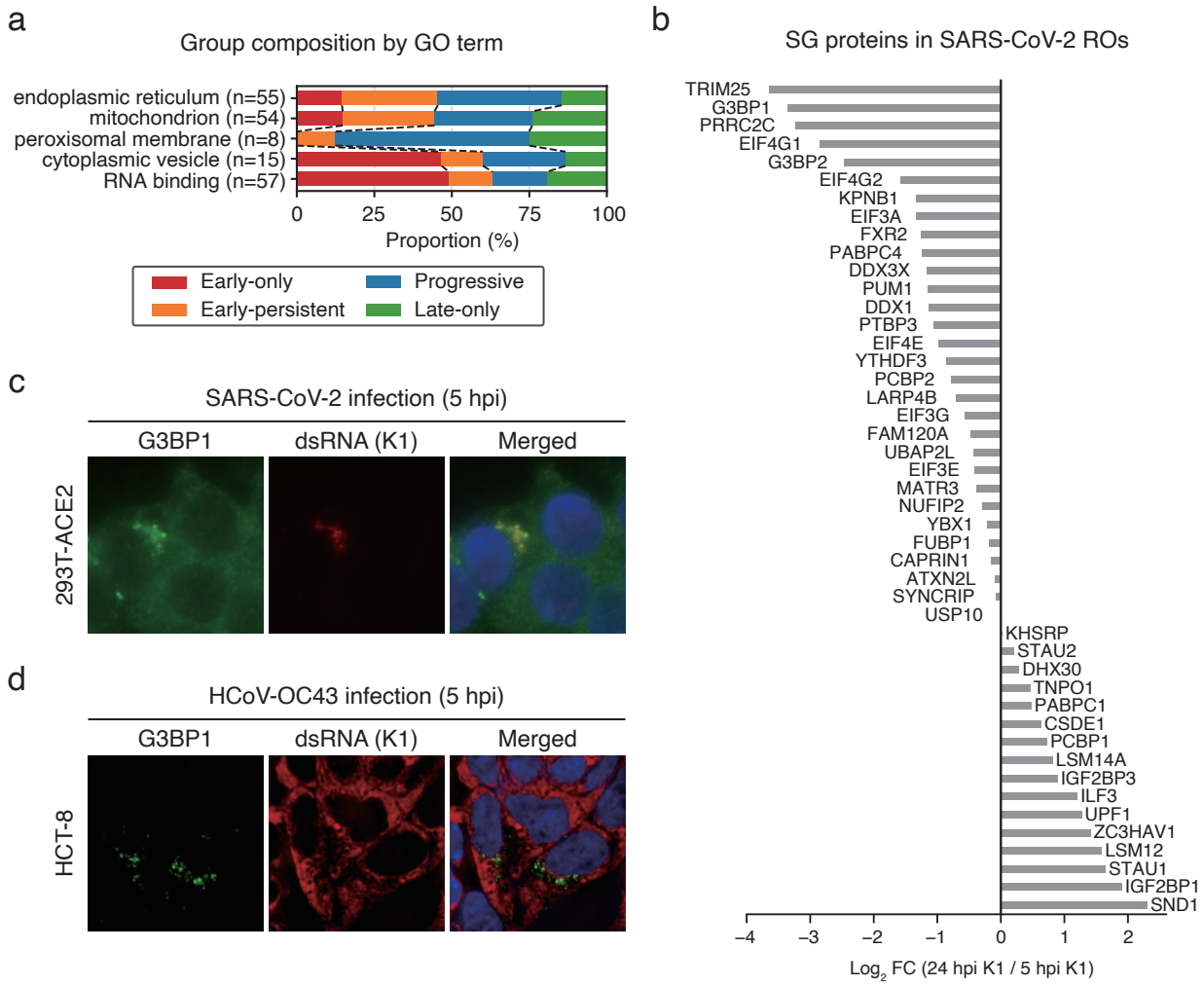

Supplementary Figure 5